Statistical Theory and Related Fields

ISSN: 2475-4269 (Print) 2475-4277 (Online) Journal homepage: www.tandfonline.com/journals/tstf20

Joint modelling accelerated life tests and field data for reliability prediction

Ancha Xu, Jiahui Liu, Lijia Liu, Mengting Zhong & Weiwei Wang

To cite this article: Ancha Xu, Jiahui Liu, Lijia Liu, Mengting Zhong & Weiwei Wang (04 May 2026): Joint modelling accelerated life tests and field data for reliability prediction, Statistical Theory and Related Fields, DOI: 10.1080/24754269.2026.2656112

To link to this article: https://doi.org/10.1080/24754269.2026.2656112

Published online: 04 May 2026.

STATISTICAL THEORY AND RELATED FIELDS
https://doi.org/10.1080/24754269.2026.2656112

Taylor & Francis
by informa

RESEARCH ARTICLE

OPEN ACCESS Check for updates

Joint modelling accelerated life tests and field data for reliability prediction

Ancha Xu[a,b], Jiahui Liu[a], Lijia Liu[a], Mengting Zhong[a] and Weiwei Wang[a]

[a]School of Statistics and Data Science, Zhejiang Gongshang University, Hangzhou, People's Republic of China; [b]Laboratory for Statistical Monitoring and Intelligent Governance of Common Prosperity, Zhejiang Gongshang University, Hangzhou, People's Republic of China

ABSTRACT

Products often operate in dynamic environments, and field failure data is frequently heavily censored, posing significant challenges in the assessment of product reliability. To enhance the accuracy of field reliability predictions, we introduce a novel joint modelling approach that combines accelerated life tests (ALT) and field failure data. We capture the stochastic influence of dynamic environmental factors on product aging using an exponential dispersion process and present a methodology for jointly modelling ALT and field failure data. Our approach is grounded in the cumulative exposure principle, providing a clear and intuitive physical interpretation. We offer point and interval estimates for model parameters and reliability using maximum likelihood and Bayesian methods, validating their effectiveness through comprehensive simulation studies. Finally, we demonstrate the performance and practical application of our proposed joint model through the analysis of a real dataset.

ARTICLE HISTORY
Received 27 July 2025
Accepted 11 January 2026

KEYWORDS
Accelerated life test; exponential dispersion process; joint model; sensitivity analysis

1. Introduction

Modern products are typically designed to meet rigorous reliability standards, making it challenging to acquire product lifespan information quickly. This poses a significant obstacle when evaluating product reliability. An effective approach to addressing this challenge is through accelerated life testing (ALT), a commonly used testing method. ALT involves subjecting the product to higher stress levels, such as elevated temperatures, increased voltage, vibration, or pressure, surpassing normal usage conditions. By accelerating the underlying failure mechanisms, ALT enables engineers to collect life data more rapidly and infer product performance under normal conditions. In this way, ALT serves as a crucial bridge between limited testing time and long-term reliability prediction, forming a cornerstone of modern reliability engineering practice.

The key areas of research in ALT encompass modelling, optimal planning, and statistical analysis, all of which have received extensive attention and have been thoroughly explored in existing literature, for example, Wayne (2004), W. Q. Meeker et al. (2021), Alhadeed and Yang (2005), Ma and Meeker (2008), Zhuang et al. (2023) and the references

CONTACT Weiwei Wang weiweiwang@mail.zjgsu.edu.cn School of Statistics and Data Science, Zhejiang Gongshang University, Hangzhou 310018, People's Republic of China

therein. Recent studies on ALT demonstrate rapid progress in both engineering applications and statistical methodology. Product-oriented research, such as cyclic-stress ALT for mechatronic products (Y. Wang et al., 2024), wind-turbine bearing life prediction (Jin et al., 2022), and LED lifetime prediction (Alsharabi et al., 2025), emphasizes developing realistic test profiles and validating acceleration factors through physical experiments and simulation. These works aim to replicate actual service environments, providing practical tools for assessing reliability when field failures are difficult to observe. Complementing these, W. B. Nelson (2024) provides a comprehensive methodological review of step- and varying-stress ALT designs, offering guidance for model selection and data analysis under cumulative exposure principles. Lamu and Yan (2024) develop classical and Bayesian reliability estimation methods for *s*-out-of-*k* systems under partially constant stress ALT with Kumaraswamy-distributed lifetimes. Mansour and Mohamed (2025) further demonstrate Bayesian estimation for step-stress ALT of electrical units, improving predictive accuracy under type-I censoring.

ALT is typically conducted under fixed environmental stress conditions, while the operational environment of a product often exhibits dynamic variability. Consequently, ALT may fail to accurately replicate the real-world operating conditions of the product in the field. Relying solely on ALT data for predicting product reliability can result in significant deviations (M. Jiang & Chen, 2015). Similarly, relying solely on field data for evaluating product reliability presents two notable drawbacks. Firstly, field data is usually heavily censored or truncated, making it challenging to handle effectively. Secondly, field data can only be collected once the product is already on the market, which may take a considerable amount of time and may lack sufficient lifetime information. In recent years, many scholars have recognized these challenges and have begun to address them by jointly modelling ALT data and field data. Liao and Elsayed (2006) utilized constant stress accelerated degradation test data to predict product reliability while assuming a dynamic operating environment for the product. W. Meeker et al. (2009) utilized survey data to determine the distribution of product usage in the field and then employed joint modelling of maintenance data and ALT data to predict product reliability, although they did not account for the dynamic characteristics of the operating environment. Pan (2010) introduced a calibration factor to describe the relationship between product lifetimes under field and accelerated stresses, enabling the joint modelling of field data and ALT data. L. Wang et al. (2013) built upon the concept of Pan (2010) and applied it to accelerated degradation data. Mittman et al. (2019) employed a Bayesian approach to hierarchically model early failures and failures due to wear. Tang et al. (2020) proposed a two-step method based on the Wiener process to effectively integrate failure time and field degradation data.

While the aforementioned studies have explored the fusion of test data and field data for modelling purposes, none of them have provided a detailed explanation of the physical mechanisms underlying the impact of dynamic environments on a product's lifespan. In other words, these models lack a comprehensive physical basis. Zheng and Xie (2008) attempted to address this by employing the proportional hazards model to illustrate the effects of dynamic usage environments. However, this model requires the inclusion of observed environmental stress data, which can be challenging to obtain during a product's usage. For instance, the life of vehicle brake pads is influenced by factors such as road conditions, driving habits, weather, and usage rates, but real-time data on these factors is often unavailable. Hence, in situations where environmental stress data is not readily accessible in the field, there is a need for a statistical model that not only provides a physical interpretation but also integrates ALT data

and field failure data to predict product reliability more accurately. To bridge this gap, our approach in this paper utilizes a class of exponential dispersion (ED) processes to capture the influence of dynamic environments on product aging. Subsequently, we establish a clear relationship between field failure data and ALT data, grounded in the cumulative exposure principle (W. Nelson, 1980). Compared to existing models, our proposed joint model offers two significant advantages. Firstly, it is highly interpretable because it effectively portrays the stochastic mechanisms governing environmental influences on product aging. Secondly, the ED process encompasses various commonly used stochastic processes as special cases, allowing us to select an 'optimal' stochastic process through data analysis. Once the stochastic mechanism is determined, the model can be employed to predict field reliability for new generations of products. Thus, our model exhibits both flexibility and scalability.

The paper is structured as follows. In Section 2, we introduce a novel model that leverages ALT and field failure data. Sections 3 and 4 are dedicated to statistical inference, where we employ both the maximum likelihood (ML) and Bayesian methods to estimate model parameters and product reliability. Subsequently, we conduct a series of simulation studies to demonstrate the effectiveness of the proposed model and inference methods in Section 5. Finally, we analyze a real-world dataset to showcase the practical application of our joint model in Section 6.

2. Models

2.1. Accelerated life test

Without loss of generality, constant stress ALT with progressive censoring is utilized in this paper, because statistical inference based on other types of ALTs and censoring schemes is similar. For the ALT model, we have the following three assumptions.

Assumption 2.1: The stress levels of the ALT are prefixed as $S_1 < S_2 < \cdots < S_m$, and n_k specimens are tested under the stress level S_k.

Assumption 2.2: Let T_k be the lifetime of product at the stress level S_k, and the cumulative distribution function (cdf) of T_k is

$$F_{\mathrm{ALT}}(t;\alpha,\eta_k) = 1 - \exp\{-\eta_k H_\alpha(t)\}, \quad k = 1,2,\ldots,m, \tag{1}$$

where η_k is the baseline failure rate, time scale transformation $H_\alpha(t)$ is a monotonically increasing function of calendar time t, and α is an unknown parameter. $H_\alpha(t)$ can be interpreted as a measure of physical aging processes such as wear, oxidation, and so on (Duchesne and Lawless (2000), Hong et al. (2019), and Xu and Wang (2026). Model (1) was first proposed by Marshall and Olkin (2007), which includes a class of commonly used lifetime distribution. Different functional forms of $H_\alpha(t)$ can lead to different lifetime distributions. For example, when $H_\alpha(t) = t^\alpha$ and $\exp(\alpha t) - 1$, T_k follows the Weibull distribution and Gompertz distribution, respectively.

Assumption 2.3: The accelerated model for lifetime and stress levels can be expressed as log-linear form. That is,

$$\log \eta_k = \gamma_0 + \gamma_1 \delta(S_k), \quad k = 0,1,2,\ldots,m, \tag{2}$$

where γ_0 and γ_1 are unknown parameters, $\delta(S)$ is a deterministic function of stress level S, and S_0 is the normal use stress level. In particular, when temperature is the stress, (2) is the

Arrhennius model, where $\delta(S) = 1/S$; when the stress is taken as the voltage, (2) is the inverse power-law model, where $\delta(S) = -\log(S)$. To simplify the notation, the following normalized transformation can be applied to $\delta(S_k)$:

$$\xi_k = \frac{\delta(S_k) - \delta(S_0)}{\delta(S_m) - \delta(S_0)}, \quad k = 0, 1, \ldots, m.$$

Therefore, the value range of ξ_k is [0,1], where $\xi_0 = 0$ and $\xi_m = 1$. Then the acceleration Equation (2) becomes

$$\log \eta_k = \beta_0 + \beta_1 \xi_k, \tag{3}$$

where $\beta_0 = \gamma_0 + \gamma_1 \delta(S_0)$ and $\beta_1 = \gamma_1(\delta(S_m) - \delta(S_0))$.

2.2. Field data modelling

Based on (1), the cdf of lifetime T at the normal use stress level S_0 is

$$F(t) = 1 - \exp\{-\eta_0 H_\alpha(t)\}. \tag{4}$$

However, the operating environment of the product is usually dynamically changing rather than a fixed stress level, which will change the aging properties of the lifetime distribution. In such a case, time scale transformation $H_\alpha(t)$ may not be deterministic. In order to characterize the effect of dynamic environment on product aging, we assume that time scale transformation is captured by a stochastic process $\{B(t), t \geq 0\}$, that is, the product aging process exhibits stochastic variations with the external environment rather than a deterministic function of time. Therefore, when the operating environment of the product has time-varying characteristics, conditioned on $\{B(t), t \geq 0\}$, the cdf of T can be expressed as

$$F(t|B(t)) = 1 - \exp\{-\eta_0 B(t)\}. \tag{5}$$

Model (5) illustrates the influence of environmental factors on product aging, and a similar approach for modelling dynamic environmental effects can also be found in Hong et al. (2019) and T. Jiang et al. (2023). In this paper, we assume that $\{B(t), t \geq 0\}$ is an ED process (Xu et al., 2021; Zhou & Xu, 2019). It has three properties: i) $B(0) = 0$; ii) it has independent increments; iii) each increment follows the ED distribution (ED $(\mu \Delta G_\alpha(t), \lambda)$) with the probability density function (pdf)

$$f_{\mathrm{ED}}(b; \theta, \lambda) = c(b, \Delta G_\alpha(t), \lambda) \exp\{\lambda [b\theta - \Delta G_\alpha(t) \kappa(\theta)]\},$$

where $\Delta G_\alpha(t) = G_\alpha(t) - G_\alpha(r)(r < t)$, $c(\cdot)$ is the canonical function, and $\kappa(\cdot)$ is the cumulant function. In addition, $\mu = \kappa'(\theta)$ is the drift parameter and λ is the dispersion parameter. When $\kappa''(\theta) = \mu^q, q \in (-\infty, 0] \cup [1, +\infty)$, the ED process includes Wiener process $(q = 0)$, Poisson process $(q = 1)$, compound Poisson process $(1 < q < 2)$, gamma process $(q = 2)$, and inverse Gaussian process $(q = 3)$ as special cases. Then $\kappa(\theta)$ has the explicit expression

$$\kappa(\theta) = \begin{cases} \exp(\theta), & q = 1, \\ -\log(-\theta), & q = 2, \\ \frac{[(1-q)\theta]^{\frac{2-q}{1-q}}}{2-q}, & q \neq 1, 2. \end{cases} \tag{6}$$

We denote the above ED process as $\mathcal{ED}(\mu G_\alpha(t), \lambda)$. Intuitively, the ED process can be viewed as a stochastic representation of cumulative product degradation under dynamic

environments. In practice, degradation accumulates over time through many small random increments caused by wear, corrosion, fatigue, or other physical mechanisms. The ED process assumes that these degradation increments follow distributions within the exponential dispersion family, such as normal, gamma, or inverse Gaussian distributions, depending on whether the degradation is monotonic, diffusive, or shock-driven. The mean component of the process describes the expected degradation trend, while the dispersion parameter quantifies the variability introduced by fluctuating operating or environmental conditions. Therefore, the ED process provides a unified framework that can capture a wide range of degradation behaviours, from steady wear to random diffusion, offering both mathematical flexibility and clear physical interpretability.

If the product is operated in a dynamic environment, based on Model (5) and the ED process $\mathcal{ED}(\mu G_\alpha(t), \lambda)$, the lifetime T can be characterized as follows:

$$\begin{cases} T|B(t) \sim F(t|B(t)), \\ B(t) \sim \mathcal{ED}(\mu G_\alpha(t), \lambda). \end{cases} \tag{7}$$

According to (7), the survival function of T is

$$\begin{aligned} R_{\mathrm{ED}}(t) &= P(T > t) = E_{B(t)}\left\{\exp\left[-\eta_0 B(t)\right]\right\} \\ &= \int \exp(-\eta_0 b) f_{\mathrm{ED}}(b; \theta, \lambda)\, \mathrm{d}b \\ &= \exp\left\{-\lambda\left[\kappa(\theta) - \kappa\left(\theta - \frac{\eta_0}{\lambda}\right)\right] G_\alpha(t)\right\} \\ &\quad \times \int c(b, G_\alpha(t), \lambda) \exp\left\{\lambda\left[b\left(\theta - \frac{\eta_0}{\lambda}\right) - G_\alpha(t)\,\kappa\left(\theta - \frac{\eta_0}{\lambda}\right)\right]\right\} \mathrm{d}b \\ &= \exp\left\{-\omega G_\alpha(t)\right\}, \end{aligned} \tag{8}$$

where $\omega = \lambda[\kappa(\theta) - \kappa(\theta - \frac{\eta_0}{\lambda})]$. Therefore, if the product is operated in a dynamic environment, the cdf of T is

$$F_{\mathrm{field}}(t; \alpha, \omega) = 1 - \exp\left\{-\omega G_\alpha(t)\right\}. \tag{9}$$

According to the cumulative exposure principle (W. Nelson, 1980), the dynamic variation in the external environment affects only the cumulative exposure of the product but does not alter the product's failure mechanism. Consequently, when comparing (4) and (9), it becomes evident that $H_\alpha(t)$ and $G_\alpha(t)$ reflect the product's failure mechanism and should be identical; in other words, $G_\alpha(t) = H_\alpha(t)$. Thus, the pdf of T in the field is

$$f_{\mathrm{field}}(t; \alpha, \omega) = \omega h_\alpha(t) \exp\left\{-\omega H_\alpha(t)\right\}, \tag{10}$$

where $h_\alpha(t)$ is the derivative of $H_\alpha(t)$ with respect to t. The impact of the operating environment on the cumulative exposure of the product is expressed through the baseline failure rate. When the stress level S_0 remains fixed, the parameter is η_0. However, when the stress level dynamically changes, the parameter becomes ω. This formulation provides a clear physical interpretation consistent with the cumulative exposure principle, enabling the model to effectively characterize and quantify the stochastic influence of environmental conditions on product degradation.

3. Maximum likelihood estimation

The observed data based on constant stress ALT is assumed to be

$$\left\{\left(y_{kj}, c_{kj}\right), k = 1, 2, \ldots, m, j = 1, 2, \ldots, n_k\right\}, \tag{11}$$

where c_{kj} is the indicator variable. If $c_{kj} = 1$, it indicates that the unit fails, and y_{kj} is the failure time in ALT. Conversely, $c_{kj} = 0$ means that y_{kj} is the censoring time in ALT. Assuming that there are n_0 units employed in the field, the observed failure data is as follows:

$$\left\{\left(x_i, c_i\right), i = 1, 2, \ldots, n_0\right\}, \tag{12}$$

where c_i is the indicator variable. If $c_i = 1$, it indicates that the unit fails in the field, and x_i represents the failure time. If $c_i = 0$, it means that the unit is censored, and x_i is the censoring time in the field. Let $\mathcal{D}$ be the set of ALT data (11) and field failure data (12). Then given $\mathcal{D}$, the likelihood function for the model parameter vector $\boldsymbol{\Omega}$ is

$$\begin{aligned} L\left(\boldsymbol{\Omega}\right) &= \prod_{k=1}^{m}\prod_{j=1}^{n_k}\left[f_{\mathrm{ALT}}\left(y_{kj}, \alpha, \eta_k\right)\right]^{c_{kj}} \times \left[1 - F_{\mathrm{ALT}}\left(y_{kj}, \alpha, \eta_k\right)\right]^{1-c_{kj}} \\ &\quad \times \prod_{i=1}^{n_0}\left[f_{\mathrm{field}}\left(x_i; \alpha, \omega\right)\right]^{c_i} \times \left[1 - F_{\mathrm{field}}\left(x_i; \alpha, \omega\right)\right]^{1-c_i} \\ &= \prod_{k=1}^{m}\prod_{j=1}^{n_k}\left[\eta_k h_\alpha\left(y_{kj}\right)\right]^{c_{kj}}\left[\mathrm{e}^{-\eta_k H_\alpha\left(y_{kj}\right)}\right]\prod_{i=1}^{n_0}\left[\omega h_\alpha\left(x_i\right)\right]^{c_i}\left[\mathrm{e}^{-\omega H_\alpha\left(x_i\right)}\right]. \end{aligned} \tag{13}$$

However, based on the likelihood function (13), it can be demonstrated that the model exhibits the issue of parameter redundancy (see the proof in Appendix 1). This implies that the parameter vector (λ, μ, q) cannot be uniquely identified. However, ω is still estimable. As suggested by Xu et al. (2021), we set $\mu = \lambda = 1$ and retain the parameter q as an unknown to circumvent the problem of parameter redundancy. The advantage of this approach lies in its versatility, where distinct values of q correspond to different stochastic processes. By estimating the parameter q, we can effectively determine the impact of the operating environment on product aging. Therefore, the model parameter vector can be denoted as $\boldsymbol{\Omega} = (\alpha, \beta_0, \beta_1, q)$.

Then, the log-likelihood function can be simplified as follows

$$\begin{aligned} \ell\left(\boldsymbol{\Omega}\right) &= N_0 \ln\omega + \sum_{i=1}^{n_0} c_i \ln h_\alpha\left(x_i\right) - \omega\sum_{i=1}^{n_0} H_\alpha\left(x_i\right) \\ &\quad + \sum_{k=1}^{m}\left[N_k \ln\eta_k + \sum_{j=1}^{n_k} c_{kj} \ln h_\alpha\left(y_{kj}\right) - \eta_k\sum_{j=1}^{n_k} H_\alpha\left(y_{kj}\right)\right], \end{aligned} \tag{14}$$

where $N_0 = \sum_{i=1}^{n_0} c_i$, $N_k = \sum_{j=1}^{n_k} c_{kj}$, $h_\alpha(y_{kj}) = \frac{\partial H_\alpha(y)}{\partial y}|_{y=y_{kj}}$ and $h_\alpha(x_i) = \frac{\partial H_\alpha(x)}{\partial x}|_{x=x_i}$. The maximum likelihood estimate (MLE) of $\boldsymbol{\Omega}$ can be obtained by maximizing $\ell(\boldsymbol{\Omega})$. In this paper, the `optim()` function in the R language is used to implement the numerical optimization calculation.

When the sample size is large enough, the MLE $\widehat{\mathbf{\Omega}}$ has asymptotic normality as follows:

$$\widehat{\mathbf{\Omega}} \sim N\left(\mathbf{\Omega}, I^{-1}\left(\mathbf{\Omega}\right)\right),$$

where $I(\mathbf{\Omega})$ is the Fisher information matrix, which is defined as

$$\begin{bmatrix} -E\left(\frac{\partial^2 l}{\partial \alpha^2}\right) & -E\left(\frac{\partial^2 l}{\partial \alpha \partial \beta_0}\right) & -E\left(\frac{\partial^2 l}{\partial \alpha \partial \beta_1}\right) & -E\left(\frac{\partial^2 l}{\partial \alpha \partial q}\right) \\ -E\left(\frac{\partial^2 l}{\partial \alpha \partial \beta_0}\right) & -E\left(\frac{\partial^2 l}{\partial {\beta_0}^2}\right) & -E\left(\frac{\partial^2 l}{\partial \beta_0 \partial \beta_1}\right) & -E\left(\frac{\partial^2 l}{\partial \beta_0 \partial q}\right) \\ -E\left(\frac{\partial^2 l}{\partial \alpha \partial \beta_1}\right) & -E\left(\frac{\partial^2 l}{\partial \beta_0 \partial \beta_1}\right) & -E\left(\frac{\partial^2 l}{\partial {\beta_1}^2}\right) & -E\left(\frac{\partial^2 l}{\partial \beta_1 \partial q}\right) \\ -E\left(\frac{\partial^2 l}{\partial \alpha \partial q}\right) & -E\left(\frac{\partial^2 l}{\partial \beta_0 \partial q}\right) & -E\left(\frac{\partial^2 l}{\partial \beta_1 \partial q}\right) & -E\left(\frac{\partial^2 l}{\partial q^2}\right) \end{bmatrix},$$

and the derivation of $I(\mathbf{\Omega})$ can be found in Appendix 2.

Let $R_{\mathrm{ED}}(t)$ be the reliability of the product at time t when it is used in the field. Then the MLE of $R_{\mathrm{ED}}(t)$ is

$$\widehat{R}_{\mathrm{ED}}(t) = \exp\left\{-\hat{\omega} H_{\hat{\alpha}}\left(t\right)\right\}, \tag{15}$$

and $\widehat{R}_{\mathrm{ED}}(t)$ is asymptotically normal distributed with mean $R_{\mathrm{ED}}(t)$ and variance $D = QI^{-1}(\mathbf{\Omega})Q^{\top}$,

$$\widehat{R}_{\mathrm{ED}}(t) \sim N(R_{\mathrm{ED}}(t), D),$$

where $Q = \left[\frac{\partial R_{\mathrm{ED}}(t)}{\partial \alpha}, \frac{\partial R_{\mathrm{ED}}(t)}{\partial \beta_0}, \frac{\partial R_{\mathrm{ED}}(t)}{\partial \beta_1}, \frac{\partial R_{\mathrm{ED}}(t)}{\partial q}\right]$ and $Q^{\top}$ is the transpose of Q. Therefore, the confidence interval (CI) of reliability can be constructed. For example, when the confidence level is 95%, the CI of R_{ED} is

$$\left(\widehat{R}_{\mathrm{ED}}(t) - Z_{0.975}\sqrt{\widehat{D}}, \widehat{R}_{\mathrm{ED}}(t) + Z_{0.975}\sqrt{\widehat{D}}\right), \tag{16}$$

where $\widehat{D}$ is the MLE of D and $Z_{0.975}$ is the 97.5% quantile of the standard normal distribution.

However, the bounds of the CI in (16) may fall outside the interval $[0, 1]$, which is not appropriate for a probability measure. Following the recommendation of W. Q. Meeker et al. (2021), a more accurate approximation can be obtained by applying the logit transformation $\mathrm{logit}(R_{\mathrm{ED}}(t)) = \log[R_{\mathrm{ED}}(t)/(1 - R_{\mathrm{ED}}(t))]$ and constructing the CI based on the asymptotic distribution of

$$R_{\mathrm{logit}(\widehat{R}_{\mathrm{ED}})} = \frac{\mathrm{logit}\left(\widehat{R}_{\mathrm{ED}}\left(t\right)\right) - \mathrm{logit}\left(R_{\mathrm{ED}}\left(t\right)\right)}{\widehat{SE}_{\mathrm{logit}(\widehat{R}_{\mathrm{ED}})}}.$$

This yields the two-sided approximate 95% CI for $R_{\mathrm{ED}}(t)$ as

$$\left(\frac{\widehat{R}_{\mathrm{ED}}(t)}{\widehat{R}_{\mathrm{ED}}(t) + (1 - \widehat{R}_{\mathrm{ED}}(t))w}, \frac{\widehat{R}_{\mathrm{ED}}(t)}{\widehat{R}_{\mathrm{ED}}(t) + (1 - \widehat{R}_{\mathrm{ED}}(t))/w}\right),$$

where $w = \exp\{Z_{0.975}\widehat{D}/[\widehat{R}_{\mathrm{ED}}(t)(1 - \widehat{R}_{\mathrm{ED}}(t))]\}$. By construction, the endpoints of this interval always lie within $(0, 1)$, ensuring that the resulting CI is consistent with the range of a reliability measure.

4. Bayesian inference

In addition to the ML method, Bayesian inference stands as a widely employed statistical approach. Within the Bayesian framework, we treat the unknown parameters as random variables. By specifying prior distributions for these parameters, we can subsequently perform inference on them through the posterior distribution. Concerning the parameters α and q, we choose uninformative priors, which are prior distributions that do not impose strong prior beliefs and are often selected to have minimal influence on the analysis. This choice is made because collecting prior information for these two parameters can be challenging in practice. For computational convenience and ease of derivation, we opt for the normal distribution as the prior distribution for β_0 and β_1. These two parameters play roles similar to regression coefficients, and the use of normal priors for regression coefficients is a common practice in generalized regression models. This choice aligns well with standard practices in Bayesian analysis (Chen & Tsui, 2013; P. Wang et al., 2018). Thus, we assign the priors of the model parameters as follows:

$$\begin{aligned}
&\pi_1(\alpha) \propto \frac{1}{\alpha}, \quad \alpha > 0,\\
&\pi_2(\beta_0) \propto \exp\left\{-\frac{(\beta_0-\mu_0)^2}{2{\sigma_0}^2}\right\}, \quad \sigma_0 > 0,\\
&\pi_3(\beta_1) \propto \exp\left\{-\frac{(\beta_1-\mu_1)^2}{2{\sigma_1}^2}\right\}, \quad \sigma_1 > 0,\\
&\pi_4(q) \propto \frac{1}{q}, \quad q > 1.
\end{aligned} \tag{17}$$

Different priors have a certain impact on the parameter estimation, and the sensitivity analysis of the priors will be discussed in the simulation. Given the prior distributions (17), the joint posterior density of the parameter vector $\boldsymbol{\Omega}$ obtained by Bayesian theorem is

$$\begin{aligned}
\pi(\boldsymbol{\Omega}|\mathcal{D}) \propto\ & \omega^{N_0} \times \prod_{i=1}^{n_0} [h_\alpha(x_i)]^{c_i} \times \exp\left(-\omega \sum_{i=1}^{n_0} H_\alpha(x_i)\right)\\
& \times \prod_{k=1}^{m}\left[{\eta_k}^{N_k} \times \prod_{j=1}^{n_k}\left[h_\alpha\left(y_{kj}\right)\right]^{c_{kj}} \times \exp\left(-\eta_k \sum_{j=1}^{n_k} H_\alpha\left(y_{kj}\right)\right)\right]\\
& \times \exp\left\{-\frac{(\beta_0-\mu_0)^2}{2{\sigma_0}^2} - \frac{(\beta_1-\mu_1)^2}{2{\sigma_1}^2}\right\} \times \frac{1}{q} \times \frac{1}{\alpha}.
\end{aligned} \tag{18}$$

Due to the complexity of the posterior density, direct computation of posterior estimates is impossible. Thus, we propose a Gibbs sampling algorithm to implement Bayesian inference. Given data $\mathcal{D}$, parameters β_0, β_1 and q, the full conditional posterior density of α,

$\pi(\alpha|\beta_0, \beta_1, q, \mathcal{D})$ is proportional to

$$\prod_{i=1}^{n_0}[h_\alpha(x_i)]^{c_i} \times \exp\left(-\omega\sum_{i=1}^{n_0}H_\alpha(x_i)\right) \times \prod_{k=1}^{m}\left[\prod_{j=1}^{n_k}\left[h_\alpha\left(y_{kj}\right)\right]^{c_{kj}} \times \exp\left(-\eta_k\sum_{j=1}^{n_k}H_\alpha\left(y_{kj}\right)\right)\right] \times \frac{1}{\alpha}, \tag{19}$$

which can be proven as a log-concave function of α when $H_\alpha(t) = t^\alpha$ and $\exp(\alpha t) - 1$ (see the proof in Appendix 3). Thus the adaptive rejection sampling (ARS) algorithm (Gilks & Wild, 1992) can be used to generate the posterior samples of α. If the log-concavity condition is not satisfied, the adaptive rejection Metropolis sampling (ARMS) method (Gilks et al., 1995) is adopted instead. Similarly, the full conditional posterior density of β_1, $\pi(\beta_1|\alpha, \beta_0, q, \mathcal{D})$ is proportional to

$$\prod_{k=1}^{m}\left[{\eta_k}^{N_k} \times \exp\left(-\eta_k\sum_{j=1}^{n_k}H_\alpha\left(y_{kj}\right)\right)\right] \times \exp\left\{-\frac{(\beta_1-\mu_1)^2}{2{\sigma_1}^2}\right\}, \tag{20}$$

which is a log-concave function of β_1. The ARS algorithm can be used to generate the posterior samples of β_1. The full conditional posterior density of β_0, $\pi(\beta_0|\alpha, \beta_1, q, \mathcal{D})$ and the full conditional posterior density of q, $\pi(q|\alpha, \beta_0, \beta_1, \mathcal{D})$ are, respectively, proportional to

$$\omega^{N_0} \times \exp\left(-\omega\sum_{i=1}^{n_0}G_\alpha(x_i)\right) \times \prod_{k=1}^{m}\left[\eta_k^{N_k} \times \exp\left(-\eta_k\sum_{j=1}^{n_k}H_\alpha\left(y_{kj}\right)\right)\right] \times \exp\left\{-\frac{(\beta_0-\mu_0)^2}{2{\sigma_0}^2}\right\} \tag{21}$$

and

$$\omega^{N_0} \times \exp\left(-\omega\sum_{i=1}^{n_0}G_\alpha(x_i)\right) \times \frac{1}{q}. \tag{22}$$

Due to the complexity of $\pi(\beta_0|\alpha, \beta_1, q, \mathcal{D})$ and $\pi(q|\alpha, \beta_0, \beta_1, \mathcal{D})$, we combines the ARS algorithm and the Metropolis-Hastings algorithm to implement the posterior sampling of β_0 and q in this paper, which can be done through the `arms()` function in the R language. The Gibbs sampling procedure can be implemented by Algorithm 1.

5. Simulation studies

5.1. Simulation studies

In this section, we validate the model and inference methods through a series of simulation studies. We assume that the product's lifetime at the normally used stress level follows a Weibull distribution, denoted as Weibull(η_0, α). The shape parameter α is set to two different values, 0.5 and 1.5, corresponding to cases of decreasing and increasing hazard functions, respectively. For the constant stress ALT, after applying a normalization transformation, we set the stress levels as $\xi_1 = 0.2$, $\xi_2 = 0.3$, and $\xi_3 = 0.5$, with the acceleration Equation (3)

Algorithm 1: Gibbs sampling algorithm

Input: Observation data $\mathcal{D}$.

Output: The point estimates and 95% CIs for parameters $\boldsymbol{\Omega}$ and reliability.

Set an initial value of $\boldsymbol{\Omega} = (\alpha, \beta_0, \beta_1, q)$, say $\boldsymbol{\Omega}^{(0)} = (\alpha^{(0)}, \beta_0^{(0)}, \beta_1^{(0)}, q^{(0)})$;

for *a in* $\{1, 2, \ldots, \mathcal{A}\}$ **do**

  Generate $\alpha^{(a)}$ based on $(\alpha^{(a-1)}, \beta_0^{(a-1)}, \beta_1^{(a-1)}, q^{(a-1)})$ from (19);

  Generate $\beta_0^{(a)}$ based on $(\alpha^{(a)}, \beta_0^{(a-1)}, \beta_1^{(a-1)}, q^{(a-1)})$ from (21);

  Generate $\beta_1^{(a)}$ based on $(\alpha^{(a)}, \beta_0^{(a)}, \beta_1^{(a-1)}, q^{(a-1)})$ from (20);

  Generate $q^{(a)}$ based on $(\alpha^{(a)}, \beta_0^{(a)}, \beta_1^{(a)}, q^{(a-1)})$ from (22);

  Calculate the reliability $R_{\mathrm{ED}}^{(a)} = \exp\{-\omega^{(a)} t^{\alpha^{(a)}}\}$.

end

Discarding the first L burn-in samples, we totally obtain $\mathcal{A} - L$ posterior samples of $(\alpha, \beta_0, \beta_1, q, R_{\mathrm{ED}})$. Then the point and interval estimates can be constructed based on the rest of $\mathcal{A} - L$ posterior samples.

taking the form $\log \eta_k = 2 + 4\xi_k$. We assume that the operating environment of the product is time-varying, and its influence on product aging is characterized by an ED process. Therefore, $B(t)$ follows an ED process, where $H_\alpha(t) = t^\alpha$. Let n_i represent the sample size at stress level ξ_i, for $i = 1, 2, 3$, and let n_0 be the sample size of field products. We consider various combinations of (n_0, n_1, n_2, n_3), as shown in Figure 1. We employ a type-II censoring scheme with an 80% censoring rate. In order to describe the different stochastic phenomena of the dynamic environment, we choose $q = 1.5$ (compound Poisson process), $q = 2$ (gamma process) and $q = 3$ (inverse Gaussian process). The field data can be generated as follows.

(1) From the acceleration equation, we know that $\log \eta_0 = 2$. Then we can obtain the value of ω when $\mu = \lambda = 1$:

$$\omega = \lambda\left[\kappa(\theta) - \kappa\left(\theta - \frac{\eta_0}{\lambda}\right)\right] = \begin{cases} 1 - \mathrm{e}^{-\eta_0}, & q = 1, \\ \log(\eta_0 + 1), & q = 2, \\ \frac{1-\left[1-\eta_0(1-q)\right]^{\frac{2-q}{1-q}}}{2-q}, & q \neq 1, 2. \end{cases}$$

(2) Generate type-II censored data from $f_{\mathrm{field}}(t; \alpha, \omega)$ in (10), which is Weibull(ω, α).

For Bayesian method, the hyperparameters in the prior distributions (17) are chosen as $\mu_0 = 4$, $\sigma_0^2 = 4$, $\mu_1 = 2$ and $\sigma_1^2 = 4$. In the Gibbs sampling algorithm, the initial values of the parameters are set as $(\alpha^{(0)}, \beta_0^{(0)}, \beta_1^{(0)}, q^{(0)}) = (2, 2, 2, 2)$. The number of iterations is 5000 and the first 1000 burn-in samples are discarded; then the remaining 4000 posterior samples are used to obtain the point estimate and 95% CI of the parameters as well as the reliability $R_{\mathrm{ED}}(t) = \exp\{-\omega t^\alpha\}$ at time point 0.1. For each combination of (α, n, q), we generate 10,000 samples from the model. For each sample, the point and 95% interval estimates of the model parameters as well as $R_{\mathrm{ED}}(0.1)$ are obtained by using the ML and Bayesian methods. To illustrate the performance of the proposed model, the product reliability is also estimated by only using ALT data, which is denoted as $R_{\mathrm{ALT}}(t)$.

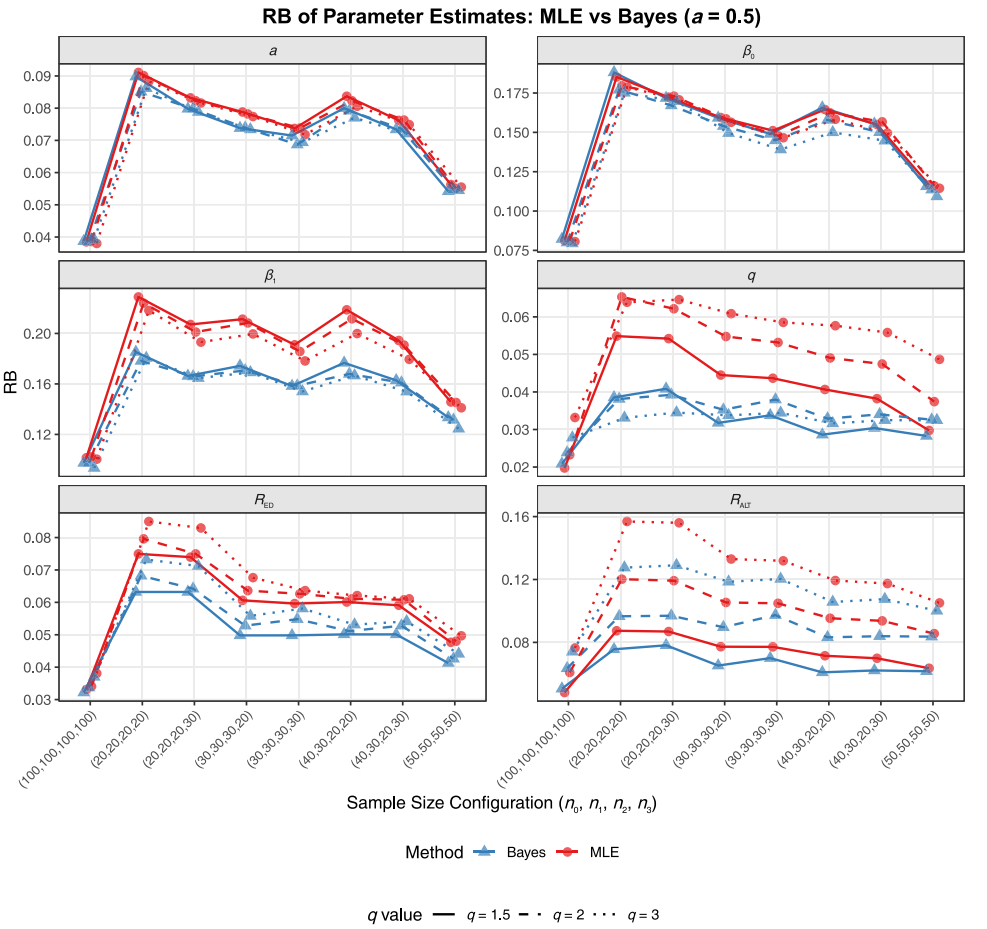

Figure 1. The RBs of point estimates of parameters and reliability when $\alpha = 0.5$.

The relative bias (RB) and root mean squared error (RMSE) of point estimates, and the coverage probability (CP) of 95% interval estimates are computed, where the RB and RMSE are calculated as follows:

$$\mathrm{RB} = \left| \frac{1}{10{,}000} \sum_{i=1}^{10{,}000} \frac{\hat{\theta}_i - \theta}{\theta} \right|, \quad \mathrm{RMSE} = \sqrt{\frac{1}{10{,}000} \sum_{i=1}^{10{,}000} \left(\hat{\theta}_i - \theta\right)^2}. \tag{23}$$

The simulation results, presented in Figures 1 to 6, reveal several key findings.

(1) As the sample size increases, both the RB and RMSE based on both methods improve, with RB gradually approaching 0 and the CP approaching the nominal level of 0.95.
(2) A comparison between the two methods indicates that the point estimates derived from the Bayesian method generally exhibit smaller RB and RMSE across most parameter settings.
(3) When considering parameters such as α, β_0, and β_1, the interval estimates based on the ML method tend to have more accurate CPs. However, for the parameter q, the interval

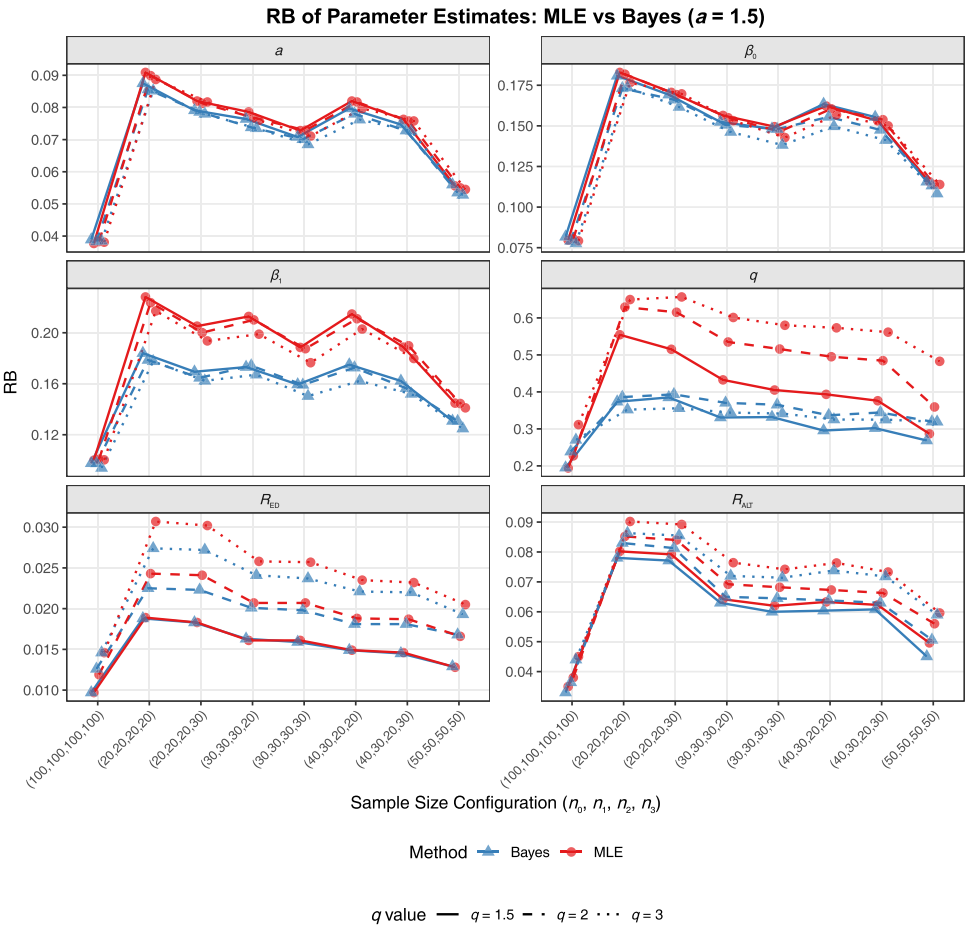

Figure 2. The RBs of point estimates of parameters and reliability when $\alpha = 1.5$.

estimates obtained through the Bayesian method are more accurate. Regarding reliability R_{ED}, the CP based on the Bayesian method outperforms the ML method in most parameter settings.

(4) Comparing the proposed joint model with the model that relies solely on ALT data, it is evident that the joint model yields significantly more accurate estimates of reliability. For instance, the RB and RMSE of R_{ED} in Figures 1 and 4 are notably smaller than those of R_{ALT}, particularly when dealing with sample sizes equal to 20 and 30. Furthermore, when considering interval estimates of reliability, the CPs based on the proposed joint model closely align with the nominal level of 0.95. Thus, the joint modelling of field data and ALT data proves to be a substantial improvement for enhancing the accuracy of reliability assessment.

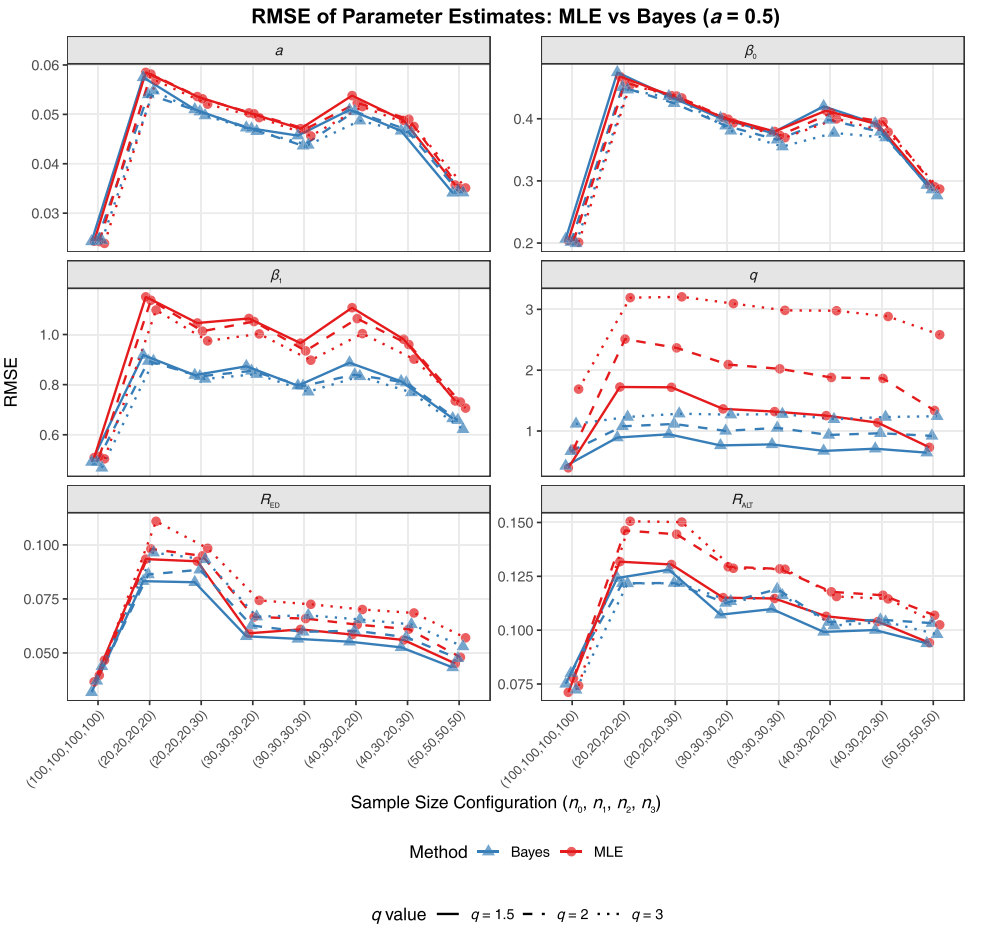

Figure 3. The RMSEs of point estimates of parameters and reliability when $\alpha = 0.5$.

5.2. Sensitivity analysis

From Section 5.1, we can see that the estimation efficiencies of both ML and Bayesian methods are close for the parameters α, β_0 and β_1, but differ significantly for the parameter q. Therefore, in this section, sensitivity analysis is performed for different prior distributions of the parameter q, and then the robustness of the Bayesian approach is investigated. Here, we only consider the case $\alpha = 1.5, q = (1.5, 2, 3)$, and the sample size $n = (30, 50, 100, 200)$. The prior distributions for the parameters α, β_0, and β_1 remain unchanged, while three prior distributions for the parameter q are considered as follows:

$$\pi_{41}(q) \propto \frac{1}{q}, \quad q > 1, \tag{24}$$

$$\pi_{42}(q) \propto q^{\mu_2 - 1} \times \exp\{-q \times \sigma_2\}, \quad q > 1, \mu_2 > 0, \sigma_2 > 0, \tag{25}$$

$$\pi_{43}(q) \propto \frac{1}{\omega}, \quad q > 1, \omega > 0. \tag{26}$$

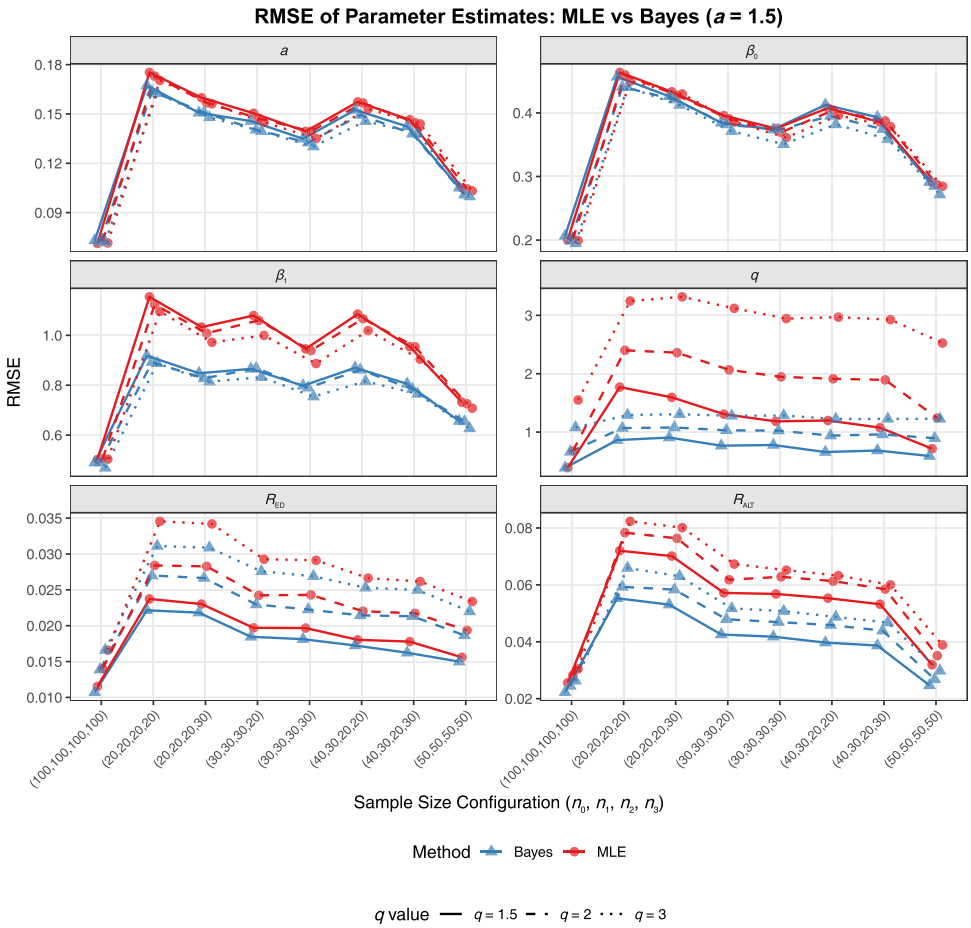

Figure 4. The RMSEs of point estimates of parameters and reliability when $\alpha = 1.5$.

The prior distribution $\pi_{41}(q)$ is the same as in Section 4 and is a non-informative prior. The prior distribution $\pi_{42}(q)$ follows gamma distribution. In the simulation, the hyperparameters μ_2 and σ_2 are set as 1 and 0.5, which means that the prior mean and variance of q are 2 and 4, respectively. Based on $\pi_{42}(q)$, the full conditional posterior density of q, $\pi_{42}(q|\alpha, \beta_0, \beta_1, \mathcal{D})$ is proportional to

$$\omega^{N_0} \times \exp\left\{-\omega \sum_{i=1}^{n_0} x_i^{\alpha}\right\} \times q^{\mu_2 - 1} \times \exp\left\{-q \times \sigma_2\right\}.$$

Posterior sampling can be implemented through the `arms()` function in the R language. The prior distribution $\pi_{43}(q)$ is also a subjective prior, and its corresponding full conditional posterior density $\pi_{43}(q|\alpha, \beta_0, \beta_1, \mathcal{D})$ is proportional to

$$\omega^{N_0 - 1} \times \exp\left\{-\omega \sum_{i=1}^{n_0} x_i^{\alpha}\right\}.$$

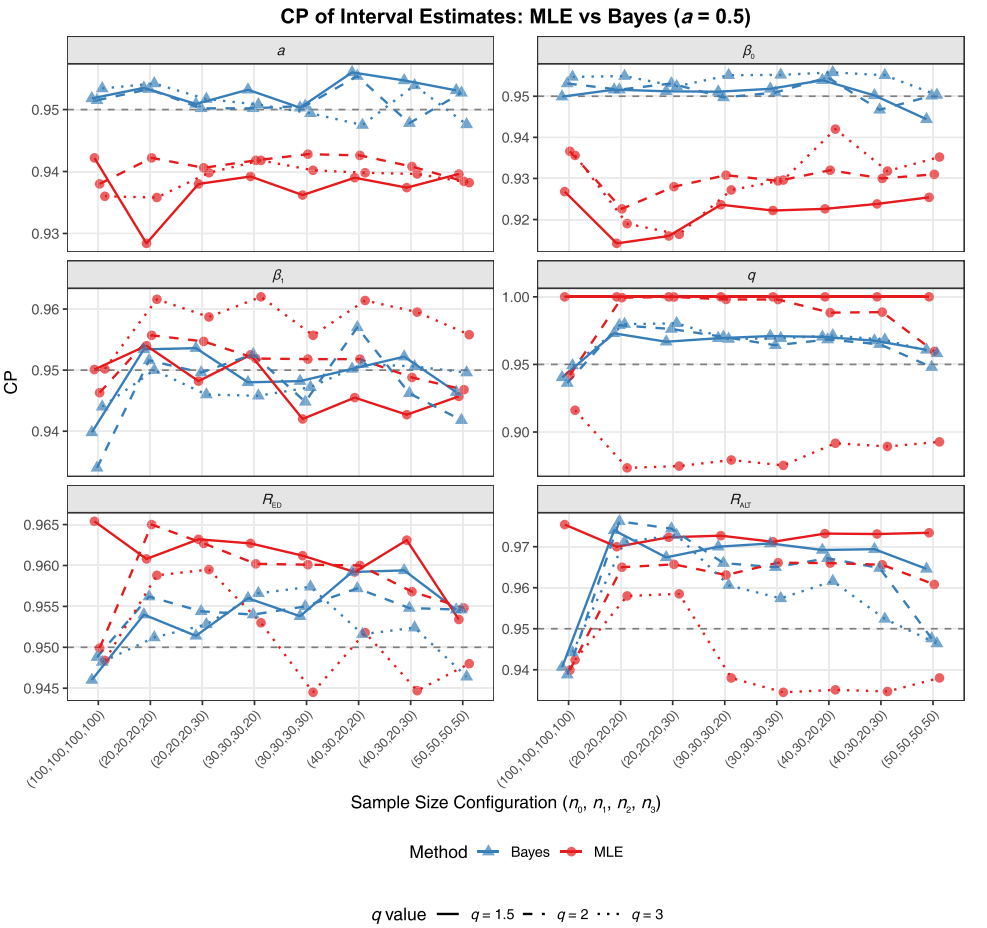

Figure 5. The CPs of interval estimates of parameters and reliability when $\alpha = 0.5$.

Then the posterior sample from $\pi_{43}(q|\alpha, \beta_0, \beta_1, \mathcal{D})$ can be generated by the rejection sampling algorithm, where the gamma distribution can be used as the instrumental distribution.

We generate 10,000 samples from the model under each parameter setting. The Bayesian point and interval estimates of parameter q are obtained, and then RB, RMSE and CP are calculated. The results are shown in Figure 7. It can be seen from Figure 7 that based on the three prior distributions, the RB and RMSE of point estimation and the CP of interval estimation are relatively close, which shows that the results are robust to prior selection.

When the sample size is $n = 50$, the true value of q is chosen from 1.5 to 3 with lag 0.075. Similarly, the experiment is repeated 10,000 times. Based on the three priors, the reliability R_{ED} is estimated, and the results are shown in Figure 8, where the red lines are the average 2.5% and 97.5% posterior quantiles, and the blue line is the average posterior mean of R_{ED}. As can be seen from Figure 8, under different priors, the posterior mean and interval estimation of R_{ED} are almost unchanged. Therefore, the prior selection of q has few effects on the reliability estimation.

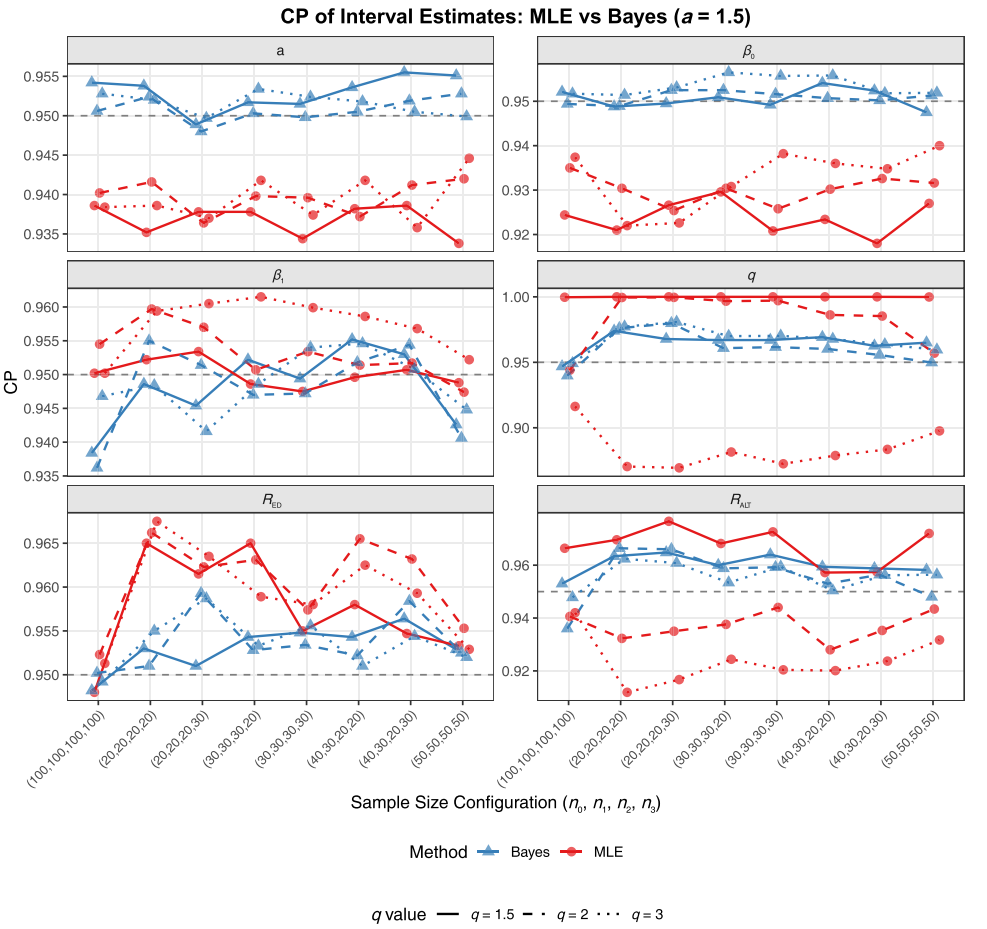

Figure 6. The CPs of interval estimates of parameters and reliability when $\alpha = 1.5$.

6. Real data analysis

In this section, the proposed model will be validated by a real case, where the data is from Fan and Yu (2013). 78 pieces of resin-coated insulation (RCI) were allocated and tested under three different temperature environments, namely, $T_1 = 195°C$, $T_2 = 220°C$ and $T_3 = 245°C$. The observed failure time is listed in Table 1. It should be noted that the dataset contains only complete failure observations, with no censored data included. To avoid arithmetic overflows, the data are divided by 90 (in quarterly time units). For illustration, we assume that $T_1 = 195°C$ is the field operating condition, and $T_2 = 220°C$ and $T_3 = 245°C$ are the stress levels of ALT. Based on the proposed model, we choose three kinds of time scale transformations: $H_\alpha(t) = \log(1 + t/\alpha), t^\alpha$ and $\exp(\alpha t) - 1$. Then the Akaike information criterion (AIC) and Bayesian information criterion (BIC) are used to select an 'optimal' time scale transformation for the data. The smaller the AIC and BIC values, the better the model fits. The results of model selection are shown in Table 2. It can be seen that when $H_\alpha(t) = t^\alpha$, the AIC and BIC values of the model are the smallest. Therefore, we use $H_\alpha(t) = t^\alpha$ to fit the data and further estimate the product reliability. We conduct a homogeneity test for the shape parameters of the three groups of data using the method described by Lawless

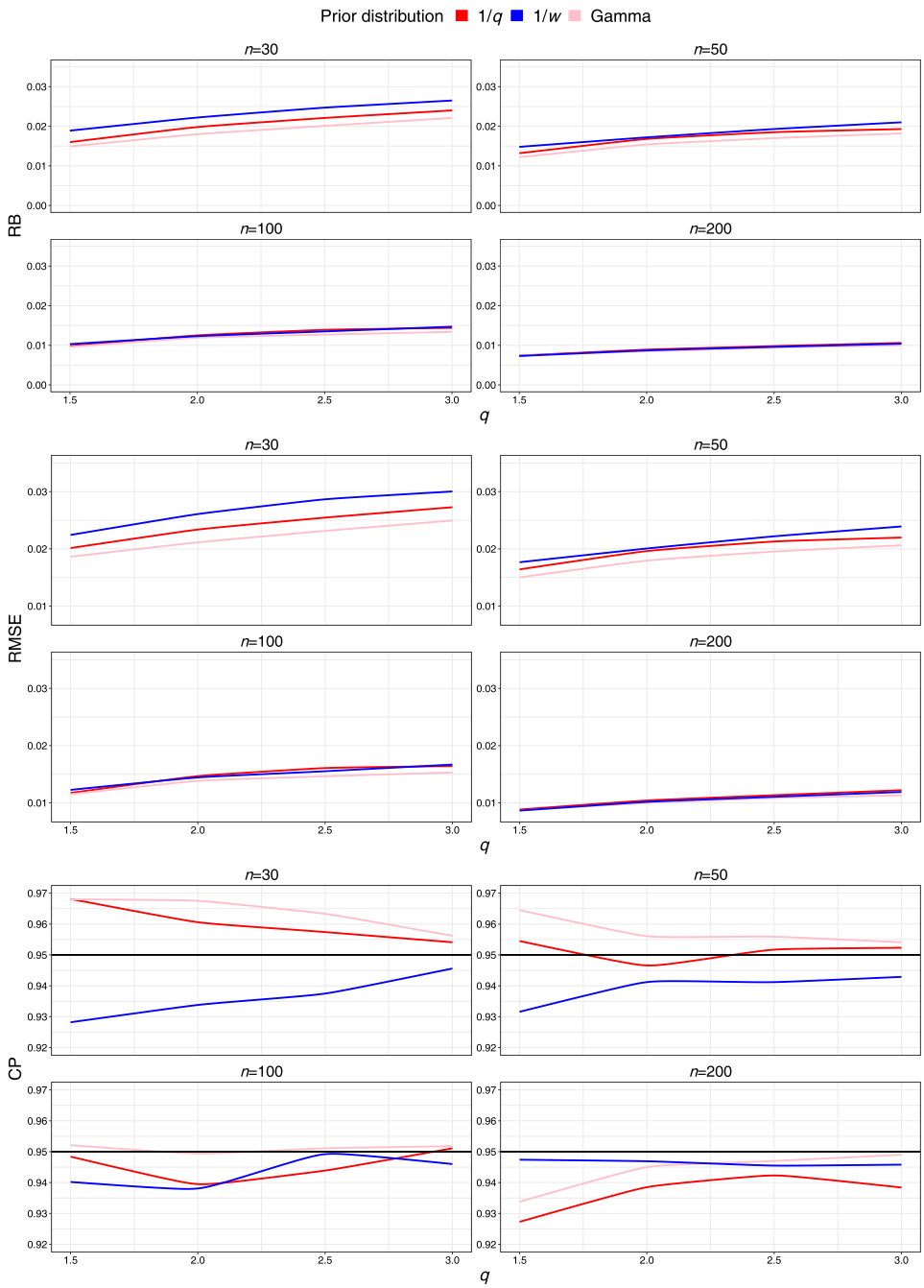

Figure 7. RB, RMSE and CP of the estimates of R_{ED} under different prior distributions.

and Mann (1976), and obtain a p-value of 0.933. Consequently, we can conclude that the shape parameters from different stress levels can be considered consistent.

To judge the convergence of Markov chains when Gibbs sampling is implemented, three different initial values are chosen for each chain, and the number of iterations is 30,000.

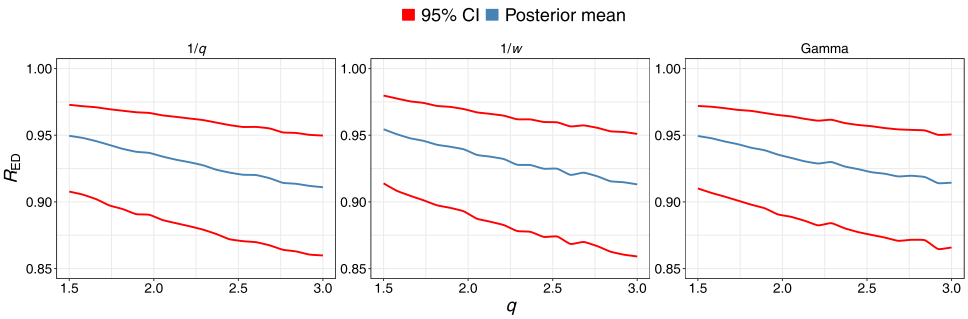

Figure 8. Effects of different priors on estimating R_{ED} ($n = 50$).

Table 1. The layout of the resin-coated insulation data.

Temperature (°C)													
195	470	482	488	500	506	518	530	536	540	548	552	556	560
	560	560	562	562	566	566	566	570	570	570	572	572	572
220	140	152	176	188	192	204	204	208	208	214	214	216	218
	218	222	222	224	224	226	228	228	230	230	234	234	236
245	66	73	87	94	94	101	101	106	106	111	111	113	113
	115	115	117	117	119	119	121	121	121	123	123	123	123

Table 2. Model selection for RCI data.

$H_\alpha(t)$	log-likelihood	AIC	BIC
t^α	**−8.3037**	**24.6074**	**33.9303**
$\exp(\alpha t) - 1$	−62.3147	132.6294	141.9523
$\log(1 + t/\alpha)$	−152.0742	312.1484	321.4713

We adopt Gelman and Rubin's convergence diagnostic method (Gelman & Rubin, 1992; Tunaru, 2002) to monitor the convergence of Markov chains. From each chain, the endpoints of the empirical $100(1-\alpha)\%$ interval are taken to get a 'within-chain' interval estimate and to calculate the potential scale reduction factor (PSRF). The results of the convergence diagnostic for each parameter are shown in Figure 9. From Figure 9, we can see that the median and 97.5% quantiles of the reduction factor tend to be 1 and reach stability after 10,000 iterations. Besides, the values of the PSRFs for all the parameters are close to 1, which indicates that the Markov chains have converged. Then the first 10,000 burn-in samples are discarded, and the remaining posterior samples are used to estimate the model parameters and the product reliability at the time point of 400 days. The point estimates and 95% interval estimates for the ML and the Bayesian methods are given in Table 3. From Table 3, we can find that R_{ALT} is much smaller than R_{ED}, and the interval estimation length of R_{ALT} is significantly larger than that of R_{ED}, which is consistent to the results in simulation studies. Thus, joint modelling can provide more lifetime information, and evaluate the reliability of product more accurate.

In addition, the estimate of q is close to 3, and it can be considered that the stochastic effects of field dynamic environment on product aging follow the inverse Gaussian process. The determination of this stochastic law is important for product reliability evaluation. For example, if the stochastic law of the field environment on product aging is known, then the

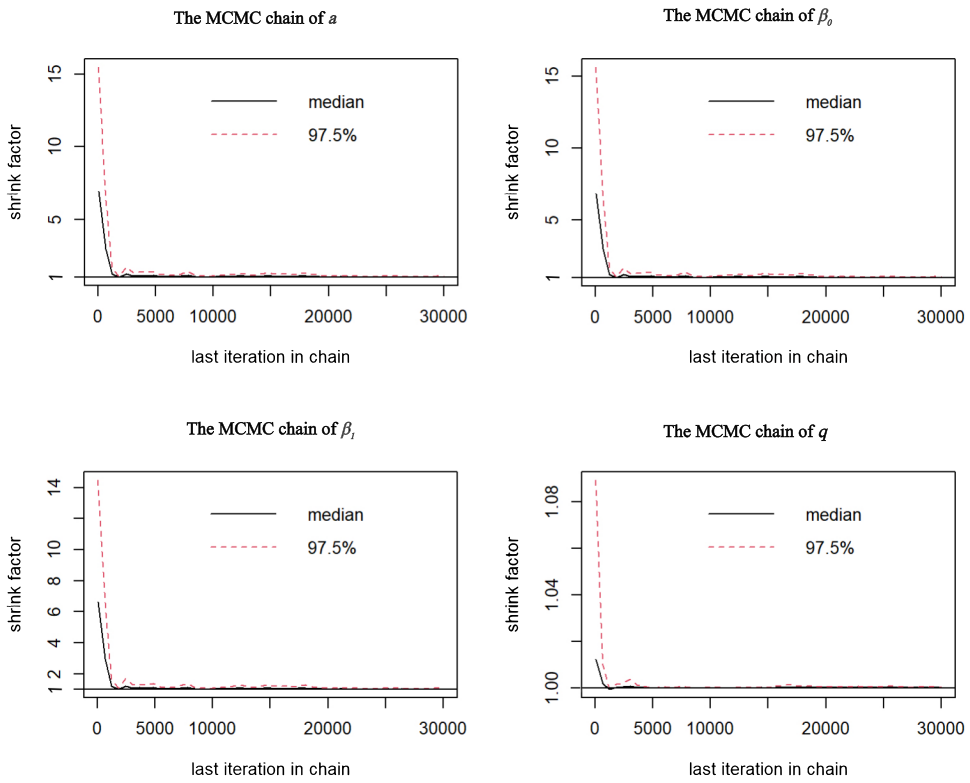

Figure 9. The Gelman-Rubin's convergence diagnostic for each parameter.

Table 3. Point estimates and 95% interval estimates of parameters and reliabilities.

	α	β_0	β_1	q	R_{ED}	R_{ALT}
MLE	11.9460	−21.4073	18.7426	3.3500	0.9580	0.7807
2.5%	10.5087	−24.0086	16.4889	1.0000	0.9198	0.5572
97.5%	13.3833	−18.8060	20.9963	7.1490	0.9823	0.9534
Bayesian	11.0532	−19.7930	17.3422	3.0920	0.9617	0.7155
2.5%	9.0598	−23.4273	14.2187	1.0491	0.9283	0.4502
97.5%	13.0360	−16.1570	20.4652	6.6545	0.9821	0.8929

lifetime distribution in the field (9) can be determined. Thus, when new generation of products is developed. the reliability of the product in the field can be predicted through ALT data, which can be used for designing warranty policy and inventory control. Compared with the assumption that the operating environment is fixed, the proposed model is more flexible and practical for field reliability prediction.

7. Conclusion

In this paper, we have introduced a novel joint model for assessing product reliability, grounded in the cumulative exposure principle. Our model integrates ALT and field data to enhance the precision of reliability estimation. Within the model, the impact of dynamic environmental factors on product aging is delineated using an ED process. We have established a clear relationship between field data and ALT data, offering a model with distinct

physical interpretations. Consequently, we have presented parameter estimation and product reliability estimation methods using both ML and Bayesian techniques. Simulation studies have demonstrated that the Bayesian approach yields more efficient parameter estimates, and these Bayesian estimates exhibit robustness to prior choice. Furthermore, through simulation studies and real data analysis, we have illustrated that our proposed joint model, in contrast to using only ALT data, offers more accurate predictions of reliability.

In practice, many modern engineering products are designed as highly reliable systems, for which field failures are rare and failure-time data are difficult to obtain within a reasonable period. In such cases, the degradation of system performance provides a more accessible and informative source for reliability assessment. The proposed ED process-based framework offers a flexible way to capture both degradation behaviour and environmental variability. In future research, integrating ALT data with field degradation information can further improve the accuracy and robustness of reliability prediction for highly reliable systems operating under dynamic conditions.

Disclosure statement

No potential conflict of interest was reported by the author(s).

Funding

The research is supported by National Natural Science Foundation of China [grant numbers 72571246, 12171432], Zhejiang Provincial Natural Science Foundation of China [grant number LZ24A010002], the Ministry of Education Humanities and Social Sciences Research Youth Project of China [grant number 25YJCZH262], the Fundamental Research Funds for the Provincial Universities of Zhejiang [grant number 2025ZDAPY01], the Summit Advancement Disciplines of Zhejiang Province (Zhejiang Gongshang University—Statistics), and Collaborative Innovation Center of Statistical Data Engineering Technology & Application.

References

Alhadeed, A. A., & Yang, S. S. (2005). Optimal simple step-stress plan for cumulative exposure model using log-normal distribution. *IEEE Transactions on Reliability*, *54*(1), 64–68. https://doi.org/10.1109/TR.2004.841704

Alsharabi, R., Almalki, L., Abed, F., Majid, M. A., & Kittaneh, O. A. (2025). A comparative analysis of statistical modeling and machine learning techniques for predicting the lifetime of light emitting diodes from accelerated life testing. *IEEE Transactions on Electron Devices*, *72*(4), 1864–1871. https://doi.org/10.1109/TED.2025.3535849

Chen, N., & Tsui, K. L. (2013). Condition monitoring and remaining useful life prediction using degradation signals: Revisited. *IIE Transactions*, *45*(9), 939–952. https://doi.org/10.1080/0740817x.2012.706376

Duchesne, T., & Lawless, J. (2000). Alternative time scales and failure time models. *Lifetime Data Analysis*, *6*(2), 157–179. https://doi.org/10.1023/A:1009616111968

Fan, T., & Yu, C. (2013). Statistical inference on constant stress accelerated life tests under generalized gamma lifetime distributions. *Quality and Reliability Engineering International*, *29*(5), 631–638. https://doi.org/10.1002/qre.v29.5

Gelman, A., & Rubin, D. B. (1992). Inference from iterative simulation using multiple sequences. *Statistical Science*, *7*(4), 457–472.

Gilks, W. R., Best, N. G., & Tan, K. K. (1995). Adaptive rejection Metropolis sampling within Gibbs sampling. *Journal of the Royal Statistical Society Series C: Applied Statistics*, *44*(4), 455–472.

Gilks, W. R., & Wild, P. (1992). Adaptive rejection sampling for Gibbs sampling. *Applied Statistics*, *41*(2), 337–348. https://doi.org/10.2307/2347565

Hong, L., Zhai, Q., Wang, X., & Ye, Z. (2019). System reliability evaluation under dynamic operating conditions. *IEEE Transactions on Reliability*, *68*(3), 800–809. https://doi.org/10.1109/TR.24

Jiang, M., & Chen, W. (2015). Integrated approach for field reliability prediction based on accelerated life testing. *Quality Engineering*, *27*(3), 317–328. https://doi.org/10.1080/08982112.2015.1036293

Jiang, T., Liu, Y., & Ye, Z. (2023). A stochastic time scale based framework for system reliability under a Markovian dynamic environment. *Naval Research Logistics*, *70*(4), 320–339. https://doi.org/10.1002/nav.22096

Jin, S., Dong, H., Chen, J., Xie, X., & Guo, M. (2022). Study on accelerated life tests for main shaft bearings in wind turbines. *Journal of Mechanical Science and Technology*, *36*(3), 1197–1207. https://doi.org/10.1007/s12206-022-0116-8

Lamu, D., & Yan, R. (2024). Reliability estimation of *s*-out-of-*k* system with Kumaraswamy distribution based on partially constant stress accelerated life tests. *Statistical Theory and Related Fields*, *8*(4), 295–314. https://doi.org/10.1080/24754269.2024.2359826

Lawless, J., & Mann, N. (1976). Tests for homogeneity of extreme value scale parameters. *Communications in Statistics-Theory and Methods*, *5*(5), 389–405. https://doi.org/10.1080/03610927608827361

Liao, H., & Elsayed, E. A. (2006). Reliability inference for field conditions from accelerated degradation testing. *Naval Research Logistics*, *53*(6), 576–587. https://doi.org/10.1002/nav.v53:6

Ma, H., & Meeker, W. Q. (2008). Optimum step-stress accelerated life test plans for log-location-scale distributions. *Naval Research Logistics (NRL)*, *55*(6), 551–562. https://doi.org/10.1002/nav.v55:6

Mansour, M. M. M., & Mohamed, N. M. (2025). Quality and reliability assessment of electrical units in accelerated life testing via Bayesian statistical approach. *Quality and Reliability Engineering International*, *41*(4), 1350–1361. https://doi.org/10.1002/qre.v41.4

Marshall, A., & Olkin, I. (2007). *Life Distributions: Structure of Nonparametric, Semiparametric, and Parametric Families*. Springer.

Meeker, W., Escobar, L., & Hong, Y. (2009). Using accelerated life tests results to predict product field reliability. *Technometrics*, *51*(2), 146–161. https://doi.org/10.1198/TECH.2009.0016

Meeker, W. Q., Escobar, L. A., & Pascual, F. G. (2021). *Statistical Methods for Reliability Data*. John Wiley & Sons.

Mittman, E., Lewis-Beck, C., & Meeker, W. (2019). A hierarchical model for heterogenous reliability field data. *Technometrics*, *61*(3), 354–368. https://doi.org/10.1080/00401706.2018.1518273

Nelson, W. (1980). Accelerated life testing step-stress models and data analysis. *IEEE Transactions on Reliability*, *29*(2), 103–108. https://doi.org/10.1109/TR.1980.5220742

Nelson, W. B. (2024). Advances in accelerated life tests with step and varying stress. *IEEE Transactions on Reliability*, *73*(1), 21–30. https://doi.org/10.1109/TR.2024.3358233

Pan, R. (2010). A Bayes approach to reliability prediction utilizing data from accelerated life tests and field failure observations. *Quality and Reliability Engineering International*, *25*(2), 229–240. https://doi.org/10.1002/qre.v25:2

Tang, S., Xu, X., Yu, C., Sun, X., Fan, H., & Si, X. S. (2020). Remaining useful life prediction with fusing failure time data and field degradation data with random effects. *IEEE Access*, *8*, 11964–11978. https://doi.org/10.1109/Access.6287639

Tunaru, R. (2002). Hierarchical Bayesian models for multiple count data. *Austrian Journal of Statistics*, *31*(3), 221–229.

Wang, L., Pan, R., Li, X., & Jiang, T. (2013). A Bayesian reliability evaluation method with integrated accelerated degradation testing and field information. *Reliability Engineering & System Safety*, *112*, 38–47. https://doi.org/10.1016/j.ress.2012.09.015

Wang, P., Tang, Y., Bae, S. J., & He, Y. (2018). Bayesian analysis of two-phase degradation data based on change-point Wiener process. *Reliability Engineering & System Safety*, *170*, 244–256. https://doi.org/10.1016/j.ress.2017.09.027

Wang, Y., Hu, J., Zhang, S., & Chen, X. (2024). Cyclic stress accelerated life test method for mechatronic products. *Quality and Reliability Engineering International*, *40*(4), 1672–1684. https://doi.org/10.1002/qre.v40.4

Wayne, N. (2004). *Accelerated Testing: Statistical Models, Test Plans, and Data Analysis*. John Wiley & Sons.

Xu, A., & Wang, W. (2026). Recursive Bayesian prediction of remaining useful life for gamma degradation process under conjugate priors. *Scandinavian Journal of Statistics*, *53*(1), 175–206. https://doi.org/10.1111/sjos.70031

Xu, A., Zhou, S., & Tang, Y. (2021). A unified model for system reliability evaluation under dynamic operating conditions. *IEEE Transactions on Reliability*, *70*(1), 65–72. https://doi.org/10.1109/TR.24
Zheng, W., & Xie, L. (2008). Dynamic reliability model of components under random load. *IEEE Transactions on Reliability*, *57*(3), 474–479. https://doi.org/10.1109/TR.2008.928184
Zhou, S., & Xu, A. (2019). Exponential dispersion process for degradation analysis. *IEEE Transactions on Reliability*, *68*(2), 398–409. https://doi.org/10.1109/TR.24
Zhuang, L., Xu, A., Wang, B., Xue, Y., & Zhang, S. (2023). Data analysis of progressive-stress accelerated life tests with group effects. *Quality Technology & Quantitative Management*, *20*(6), 763–783. https://doi.org/10.1080/16843703.2022.2147690

Appendices

Appendix 1. Non-identifiability of the parameters

In the likelihood function (13), the parameters λ, μ, and q appear only in the term

$$\prod_{i=1}^{n_0} [\omega h_\alpha(x_i)]^{c_i} \exp\{-\omega H_\alpha(x_i)\},$$

where $\omega = \lambda[\kappa(\theta) - \kappa(\theta - \frac{\eta_0}{\lambda})]$. The parameter ω can be estimated by

$$\hat{\omega} = \frac{\sum_{i=1}^{n_0} c_i}{\sum_{i=1}^{n_0} H_{\hat{\alpha}}(x_i)},$$

where $\hat{\alpha}$ denotes the MLE of α. Since λ, μ, and q enter the likelihood function only through the composite term ω, they are not separately identifiable. This leads to a parameter redundancy problem, meaning that different combinations of (λ, μ, q) can yield the same likelihood value.

Appendix 2. Fisher information matrix of Ω

The second-order partial derivatives of the log-likelihood function are as follows:

$$\frac{\partial^2 l}{\partial \alpha^2} = -\sum_{i=1}^{n_0} c_i \times \frac{\left[h'_\alpha(x_i)\right]^2 - h''_\alpha(x_i)\, h_\alpha(x_i)}{h_\alpha^2(x_i)} - \omega \sum_{i=1}^{n_0} H''_\alpha(x_i)$$
$$- \sum_{k=1}^{m} \left\{ \sum_{j=1}^{n_k} c_{kj} \times \frac{\left[h'_\alpha(y_{kj})\right]^2 - h''_\alpha(y_{kj})\, h_\alpha(y_{kj})}{h_\alpha^2(y_{kj})} + \eta_k \sum_{j=1}^{n_k} H''_\alpha(y_{kj}) \right\},$$

$$\frac{\partial^2 l}{\partial {\beta_0}^2} = -\frac{N_0}{\omega^2} \times \left(\frac{\partial \omega}{\partial \beta_0}\right)^2 + \left(\frac{N_0}{\omega} - \sum_{i=1}^{n_0} H_\alpha(x_i)\right) \times \frac{\partial^2 \omega}{\partial {\beta_0}^2} - \sum_{k=1}^{m} \left(\eta_k \sum_{j=1}^{n_k} H_\alpha(y_{kj})\right),$$

$$\frac{\partial^2 l}{\partial {\beta_1}^2} = -\sum_{k=1}^{m} \left(\eta_k S_k^2 \sum_{j=1}^{n_k} H_\alpha(y_{kj})\right),$$

$$\frac{\partial^2 l}{\partial q^2} = -\frac{N_0}{\omega^2} \times \left(\frac{\partial \omega}{\partial q}\right)^2 + \left(\frac{N_0}{\omega} - \sum_{i=1}^{n_0} H_\alpha(x_i)\right) \times \frac{\partial^2 \omega}{\partial q^2},$$

$$\frac{\partial^2 l}{\partial \alpha \partial \beta_0} = -\frac{\partial \omega}{\partial \beta_0} \times \sum_{i=1}^{n_0} H'_\alpha(x_i) - \sum_{k=1}^{m} \left(\eta_k \sum_{j=1}^{n_k} H'_\alpha(y_{kj})\right),$$

$$\frac{\partial^2 l}{\partial \alpha \partial \beta_1} = -\sum_{k=1}^{m} \left(\eta_k S_k \sum_{j=1}^{n_k} H'_\alpha(y_{kj})\right),$$

$$\frac{\partial^2 l}{\partial\alpha\partial q} = -\frac{\partial\omega}{\partial q}\times\sum_{i=1}^{n_0} H'_{\alpha}(x_i),$$

$$\frac{\partial^2 l}{\partial\beta_0\partial\beta_1} = -\sum_{k=1}^{m}\left(\eta_k S_k\sum_{j=1}^{n_k} H_{\alpha}(y_{kj})\right),$$

$$\frac{\partial^2 l}{\partial\beta_0\partial q} = -\frac{N_0}{\omega^2}\times\frac{\partial\omega}{\partial q}\times\frac{\partial\omega}{\partial\beta_0}+\left(\frac{N_0}{\omega}-\sum_{i=1}^{n_0} H_{\alpha}(x_i)\right)\times\frac{\partial^2\omega}{\partial\beta_0\partial q},$$

$$\frac{\partial^2 l}{\partial\beta_1\partial q} = 0, \tag{A1}$$

where

$$\frac{\partial\omega}{\partial\beta_0} = \begin{cases} \eta_0 e^{-\eta_0}, & q=1,\\ -\frac{\eta_0}{1+\eta_0}, & q=2,\\ \eta_0 A^{\frac{1}{1-q}}, & q\neq 1,2,\end{cases}$$

$$\frac{\partial^2\omega}{\partial{\beta_0}^2} = \begin{cases} \eta_0 e^{-\eta_0}(1-\eta_0), & q=1,\\ -\frac{\eta_0}{(1+\eta_0)^2}, & q=2,\\ \eta_0\times A^{\frac{1}{1-q}}\times\left(1-\frac{1}{A}\right), & q\neq 1,2,\end{cases}$$

$$\frac{\partial^2\omega}{\partial\beta_0\partial q} = \begin{cases} 0, & q=1 \text{ or } 2,\\ \eta_0\times A^{\frac{1}{1-q}}\times\left[\frac{1}{(1-q)^2}\times\ln A+\frac{1}{1-q}\times\frac{\eta_0}{A}\right], & q\neq 1,2,\end{cases}$$

$$\frac{\partial\omega}{\partial q} = \frac{-A^{\frac{2-q}{1-q}}\times(2-q)\times B+1-A^{\frac{2-q}{1-q}}}{(2-q)^2},$$

$$\frac{\partial^2\omega}{\partial q^2} = -\frac{(2-q)\times\left(A^{\frac{2-q}{1-q}}\times B^2+A^{\frac{2-q}{1-q}}\times\frac{\partial B}{\partial q}\right)+2\times B\times A^{\frac{2-q}{1-q}}}{(2-q)^2} + \frac{2\times\left(1-A^{\frac{2-q}{1-q}}\right)}{(2-q)^3},$$

$$h'_{\alpha}(y_{kj}) = \frac{\partial h_{\alpha}(y)}{\partial\alpha}\Big|_{y=y_{kj}}, h''_{\alpha}(y_{kj}) = \frac{\partial h^2{}_{\alpha}(y)}{\partial\alpha^2}\Big|_{y=y_{kj}},$$

$$h'_{\alpha}(x_i) = \frac{\partial h_{\alpha}(x)}{\partial\alpha}\Big|_{x=x_i}, h''_{\alpha}(x_i) = \frac{\partial h^2{}_{\alpha}(x)}{\partial\alpha^2}\Big|_{x=x_i},$$

$$H'_{\alpha}(x_i) = \frac{\partial H_{\alpha}(x)}{\partial\alpha}\Big|_{x=x_i}, H''_{\alpha}(x_i) = \frac{\partial H^2{}_{\alpha}(y)}{\partial\alpha^2}\Big|_{x=x_i},$$

$$H'_{\alpha}(y_{kj}) = \frac{\partial H_{\alpha}(y)}{\partial\alpha}\Big|_{y=y_{kj}}, H''_{\alpha}(y_{kj}) = \frac{\partial H^2{}_{\alpha}(y)}{\partial\alpha^2}\Big|_{y=y_{kj}},$$

$$A = 1-\eta_0(1-q), B = \frac{1}{(2-q)^2}\times\ln A+\frac{2-q}{1-q}\times\frac{\eta_0}{A},$$

$$\frac{\partial B}{\partial q} = \frac{2\ln A}{(1-q)^3}+\frac{2\eta_0}{(1-q)^2 A}-\frac{2-q}{1-q}\times\frac{\eta_0^2}{A^2}.$$

Thus, if the expression of $H_\alpha(t)$ is known, the Fisher information matrix $I(\boldsymbol{\Omega})$ is

$$\begin{bmatrix} -E\left(\frac{\partial^2 l}{\partial \alpha^2}\right), & -E\left(\frac{\partial^2 l}{\partial \alpha \partial \beta_0}\right) & -E\left(\frac{\partial^2 l}{\partial \alpha \partial \beta_1}\right) & -E\left(\frac{\partial^2 l}{\partial \alpha \partial q}\right) \\ -E\left(\frac{\partial^2 l}{\partial \alpha \partial \beta_0}\right) & -E\left(\frac{\partial^2 l}{\partial {\beta_0}^2}\right) & -E\left(\frac{\partial^2 l}{\partial \beta_0 \partial \beta_1}\right) & -E\left(\frac{\partial^2 l}{\partial \beta_0 \partial q}\right) \\ -E\left(\frac{\partial^2 l}{\partial \alpha \partial \beta_1}\right) & -E\left(\frac{\partial^2 l}{\partial \beta_0 \partial \beta_1}\right) & -E\left(\frac{\partial^2 l}{\partial {\beta_1}^2}\right) & -E\left(\frac{\partial^2 l}{\partial \beta_1 \partial q}\right) \\ -E\left(\frac{\partial^2 l}{\partial \alpha \partial q}\right) & -E\left(\frac{\partial^2 l}{\partial \beta_0 \partial q}\right) & -E\left(\frac{\partial^2 l}{\partial \beta_1 \partial q}\right) & -E\left(\frac{\partial^2 l}{\partial q^2}\right) \end{bmatrix}.$$

Appendix 3. Log-concavity of full conditional posterior of α

(I) When $H_\alpha(t) = t^\alpha$, then $h_\alpha(t) = \alpha t^{\alpha-1}$. Thus, (19) is reduced to be

$$Q_1(\alpha) = \alpha^{\sum_{i=1}^{n_0} c_i + \sum_{k=1}^{m}\sum_{j=1}^{n_k} c_{kj} - 1} \left(\prod_{i=1}^{n_0} x_i \prod_{k=1}^{m}\prod_{j=1}^{n_k} y_{kj}\right)^{\alpha-1} \times \exp\left(-\omega \sum_{i=1}^{n_0} x_i^\alpha - \sum_{k=1}^{m} \eta_k \sum_{j=1}^{n_k} y_{kj}^\alpha\right).$$

Taking the second derivation of $\ln Q_1(\alpha)$ yields

$$-\frac{\sum_{i=1}^{n_0} c_i + \sum_{k=1}^{m}\sum_{j=1}^{n_k} c_{kj} - 1}{\alpha^2} - \omega \sum_{i=1}^{n_0} x_i^\alpha [\ln x_i]^2 - \sum_{k=1}^{m} \eta_k \sum_{j=1}^{n_k} y_{kj}^\alpha [\ln y_{kj}]^2 < 0.$$

(II) When $H_\alpha(t) = \exp(\alpha t) - 1$, then $h_\alpha(t) = \alpha \exp(\alpha t)$. Thus, (19) is reduced to be

$$Q_2(\alpha) = \alpha^{\sum_{i=1}^{n_0} c_i + \sum_{k=1}^{m}\sum_{j=1}^{n_k} c_{kj} - 1} \exp\left(\alpha \sum_{i=1}^{n_0} c_i x_i + \alpha \sum_{k=1}^{m}\sum_{j=1}^{n_k} c_{kj} y_{kj}\right) \times \exp\left(-\omega \sum_{i=1}^{n_0} [\exp(\alpha x_i) - 1] - \sum_{k=1}^{m} \eta_k \sum_{j=1}^{n_k} [\exp(\alpha y_{kj}) - 1]\right).$$

Taking the second derivation of $\ln Q_2(\alpha)$ yields

$$-\frac{\sum_{i=1}^{n_0} c_i + \sum_{k=1}^{m}\sum_{j=1}^{n_k} c_{kj} - 1}{\alpha^2} - \omega \sum_{i=1}^{n_0} x_i^2 \exp(\alpha x_i) - \sum_{k=1}^{m} \eta_k \sum_{j=1}^{n_k} y_{kj}^2 \exp(\alpha y_{kj}) < 0.$$